OPEN ACCESS Freely available online
http://www.banglajol.info/index.php/BJID/index
Original Article
Bangladesh Journal of Infectious Diseases
December 2025, Volume 12, Number 2, Page 273-284
ISSN (Online) 2411-670X
ISSN (Print) 2411-4820
NLM ID: 101761093
DOI: https://doi.org/10.3329/bjid.v12i2.85464

Development and Evaluation of Fluorogenic and Chromogenic Chitosan-Based Hydrogels for the Detection of Bacterial Enzymes

Kausain Akther[1], Md Al Amin[2], Fariya Khan Sharna[3], Aminul Islam[4], Md Samiul Bashir[5], Anika Zafreen[6], Md. Ashiqur Rahman[7], Arifa Akram[8]

[1]Undergraduate Student, Department of Pharmacy, East West University, Dhaka, Bangladesh; [2]Graduate Research Assistant, Department of Applied Chemistry and Chemical Engineering, University of Rajshahi, Rajshahi, Bangladesh; [3]Reseaerch Assistant, Department of Emerging Infections, International Centre for Diarrhoeal Disease Research, Dhaka, Bangladesh; [4]Undergraduate Student, Department of Pharmacy, East West University, Dhaka, Bangladesh; [5]Lecturer, Department of Laboratory Medicine, Institute of Health Technology, Kurigram, Bangladesh; [6]Senior Officer, Department of Quality Assurance, Novus Clinical Research Services Limited, Dhaka, Bangladesh; [7]Officer, Deparment of Laboratory Medicine, Novus Clinical Research Services Limited, Dhaka, Bangladesh; [8]Assistant Professor, Department of Virology, National Institute of Laboratory Medicine and Referral Centre, Dhaka, Bangladesh

Abstract

Background: Chitosan hydrogels are biocompatible, biodegradable, and pH-sensitive. Grafting them with fluorogenic and chromogenic substrates allows rapid in-situ detection of bacterial enzymes via fluorescence and absorbance, offering a faster alternative to traditional methods. **Objective:** The aim of this study was to develop and evaluate fluorogenic and chromogenic chitosan hydrogels for rapid detection of α-glucosidase and β-galactosidase and assess pH effects on their enzyme responses. **Methodology:** This study was conducted at the Department of Pharmacy, East West University, Dhaka, Bangladesh (Feb–Dec 2019). Chitosan-based hydrogels were prepared and grafted with fluorogenic (MUD) and chromogenic (X-GAL) substrates to detect α-glucosidase and β-galactosidase. Films were formed on silicon wafers and modified via EDC/NHS coupling. Enzyme reactions, pH effects, and hydrogel stability were evaluated using fluorescence and absorbance measurements. **Results:** The enzymatic reaction of MUD-grafted NSC with α-glucosidase released 4-methylumbelliferone (4-MU), showing strong fluorescence at 450 nm, which increased with dye concentration and was highly pH-dependent. Kinetic studies revealed that 4-MU production was fastest at pH 6.0 and slowest at pH 8.0, with maximum concentrations of 20.6 µM, 11.2 µM, and 1.68 µM at pH 6.0, 7.0, and 8.0, respectively. X-GAL-modified NSC hydrogels reacted with β-galactosidase to release a visible blue dye, with absorbance peaks at 650 nm. Aging studies showed that sterilized hydrogels exhibited 44% dye loss over 4 weeks, while non-sterilized hydrogels showed only 17.2% loss, indicating better retention of enzymatic activity in non-sterilized samples. **Conclusion:** Fluorogenic and chromogenic chitosan-based hydrogels effectively detect bacterial enzymes α-glucosidase and β-galactosidase. The enzymatic responses are strongly influenced by pH, and the hydrogels maintain functionality for up to 4 weeks, demonstrating potential for rapid in-situ bacterial detection. [*Bangladesh Journal of Infectious Diseases, December 2025;12(2):273-284*]

Keywords: Chitosan hydrogel; Fluorogenic dye; Chromogenic dye; Enzyme detection; β-GAL & α-GLU

Correspondence: Dr Arifa Akram, Assistant Professor, Department of Virology, National Institute of Laboratory Medicine and Referral Centre, Dhaka, Bangladesh, Email: drbarna43@gmail.com, Orchid id: 0000-0001-8829-9817; Mobile: 01816296249

Introduction

The recent advancements in biomedical technologies such as wound dressings, tissue engineering, and controlled drug release systems have significantly increased the demand for biodegradable polymers[1]. These polymers can be tailored to exhibit desirable physicochemical properties, enhancing their performance in biomedical applications. Consequently, research in this area has become increasingly focused on improving the compatibility of biodegradable polymers with the human physiological system[2].

In particular, biodegradable hydrogels such as chitosan and collagen have gained attention for their potential in *in-situ* detection of bacteria and enzymes. This property can be exploited to develop infection-sensing wound dressings, which are of great importance in clinical care. Traditional bacterial detection methods rely on culturing microorganisms on agar plates, which, although reliable, are time-consuming and labor-intensive[3]. Since early detection of pathogenic bacteria is crucial in preventing disease transmission, there is a growing need for inexpensive, rapid, and easy-to-use diagnostic systems. Several modern approaches address this need by integrating enzyme-responsive materials that generate detectable optical signals in response to bacterial activity[4].

Previous studies have demonstrated that bacterial enzymes can be detected through optical methods using fluorogenic or chromogenic substrates[5,6]. For instance, chitosan hydrogels modified with such substrates can produce measurable fluorescence or color changes upon enzymatic hydrolysis. Chitosan, a naturally derived amino polysaccharide obtained by partial deacetylation of chitin, is one of the most widely used polymers in this context due to its biodegradability, biocompatibility, and pH sensitivity. Its derivatives have been successfully applied in wound healing, tissue engineering, and biosensing applications[7].

Fluorogenic and chromogenic substrates such as 4-methylumbelliferyl α-D-glucopyranoside (MUD) and 5-bromo-4-chloro-3-indolyl-β-D-galactopyranoside (X-GAL) have shown promise for detecting the enzymatic activities of α-glucosidase and β-galactosidase, respectively[8]. These enzyme-responsive systems allow real-time monitoring of bacterial presence through measurable fluorescence or colorimetric responses, providing a foundation for the development of rapid biosensors[9]. The aim of this study is to develop and evaluate fluorogenic and chromogenic chitosan-based hydrogels for the rapid detection of bacterial enzymes α-glucosidase and β-galactosidase, and to investigate the effect of pH on their enzyme-responsive behavior.

Methodology

Study Place and Duration: This experimental study was conducted at the Department of Pharmacy, East West University, Dhaka, Bangladesh, from February 2019 to December 2019. The research focused on the development and evaluation of chitosan-based hydrogels for the detection of bacterial enzymes.

Materials: Silicon (100) wafers with native oxide layers were used as substrates for hydrogel preparation. Chitosan (medium molecular weight, 75–85% deacetylated), 4-Methylumbelliferone (4-MU), 4-Methylumbelliferyl α-D-glucopyranoside (MUD), 5-Bromo-4-chloro-3-indolyl-β-D-galactopyranoside (X-GAL), α-Glucosidase (from *Saccharomyces cerevisiae*), β-Galactosidase (from *E. coli*), EDC·HCl, NHS, succinic anhydride, MES hydrate, and phosphate-buffered saline (PBS, pH 7.4) were obtained from Sigma-Aldrich. Analytical-grade acetic acid, acetone, DMSO, HCl, NaOH, and ethanol were obtained from standard suppliers. Milli-Q water (18.0 MΩ·cm) was used throughout. A UV–ozone cleaner and ultrasonic bath were employed for substrate cleaning. Black and transparent 96-well microplates were used for hydrogel fabrication and enzyme assays.

Preparation of Chitosan and NSC Solutions: A 1.0% (w/v) chitosan solution was prepared by dissolving chitosan in 1.0 wt% acetic acid under mild stirring overnight and filtered through Whatman grade 5 paper. N-succinyl chitosan (NSC) was synthesized by reacting chitosan with succinic anhydride in DMSO at 60 °C for 24 h, followed by purification through washing, precipitation, and drying under vacuum at 50 °C. A 0.7 wt% NSC solution was prepared by dissolving the purified product in Milli-Q water with vigorous stirring.

Preparation of Buffers and Reagents: Acidified water (1.0 wt% acetic acid), PBS (pH 7.4), MES buffer (pH 5.5–6.0), and NaOH/HCl stock solutions were prepared according to standard protocols. PBS solutions of varying pH (6.0–8.0) were adjusted using NaOH or HCl based on the Henderson–Hasselbalch equation. Stock 4-MU solution (1 mM in ethanol) was serially diluted to 1–5 μM in PBS (pH 6.0, 7.0, 8.0). For pH variation experiments, 4-MU (5 μM) was prepared in PBS at pH 5.5–8.0.

Enzyme solutions (0.2 μM) of α-Glucosidase and β-Galactosidase were prepared in PBS at appropriate pH values for kinetic and aging studies, respectively[10].

Preparation of Chitosan and NSC Films: Silicon wafers (1 × 1 cm²) were cleaned by sequential sonication in 70% ethanol and Milli-Q water, dried with nitrogen, and treated with UV–ozone for 30 min. Films of chitosan and NSC were prepared by drop-casting 108 μL of respective solutions onto the wafers and drying overnight in a vacuum oven at 40^0 C.

Characterization of Films and Preparation of 96-Well Plates: Fourier Transform Infrared Spectroscopy (FTIR) was performed using a Bruker TENSOR 27 spectrometer equipped with a diamond ATR accessory. Spectra were recorded between 600–4000 cm^{-1} (150 scans) and analyzed for characteristic functional group peaks. One black and two transparent 96-well plates were used for fluorescence and aging experiments, respectively. The transparent plates were sterilized using gamma irradiation. NSC solution (100 μL, 0.7 wt%) was added to designated wells and air-dried under a clean hood for 1–2 days

Modification of NSC Hydrogels: Hydrogels were grafted using EDC/NHS coupling. NSC films were first activated with EDC (30 mM) and NHS (30 mM) in MES buffer for 1.5 h, then reacted with MUD (2.5 mM in DMSO–MES, 1:4) for 6 h under dark conditions. The films were washed thoroughly with Milli-Q water and dried overnight. For X-GAL modification, a similar procedure was followed using X-GAL (2.5 mM) instead of MUD.

Calibration, Fluorescence Measurements and Kinetic Studies: For calibration, black 96-well plates were prepared with 4-MU solutions of known concentrations in PBS at different pH values. Fluorescence was measured using an Infinite F200 PRO microplate reader (Tecan, Austria) under optimized excitation and emission parameters. Background fluorescence from PBS-only wells was subtracted from each measurement.

For additional validation, 4-MU fluorescence spectra were recorded using a Varian Cary Eclipse spectrometer (scan rate = 600 nm/min; slit width = 5 nm) in PBS at pH 6.0, 7.0, and 8.0. The enzymatic reaction between α-Glucosidase (0.2 μM) and MUD-grafted NSC (5 mg) was monitored for 180 min at pH 6.0, 7.0, and 8.0. Fluorescence intensity was recorded every 2 min and plotted as concentration of 4-MU versus reaction time to evaluate kinetics[11].

Aging Studies of X-GAL Modified NSC Hydrogels: To assess the stability of the X-GAL-modified hydrogel, β-Galactosidase (0.2 μM) was added to the test wells, and PBS was added to control wells. Absorbance and color changes were measured immediately and after incubation at 37 °C for 2 and 4 weeks. UV–visible spectra were recorded to evaluate the retention of enzymatic activity over time.

Results

Investigation of Response of 4-MU using Microplate Reader: The modification of chitosan to NSC and the grafting of either MUD or X-GAL to NSC are reactions, in which an acid group is converted to an amine by the formation of an amide bond. Moreover, the condensation reaction between the carboxylic acid group of NSC and the alcohol group of MUD results in the formation of an ester group. Both the amide bond and ester bond can be detected by ATR-FTIR (Figure I).

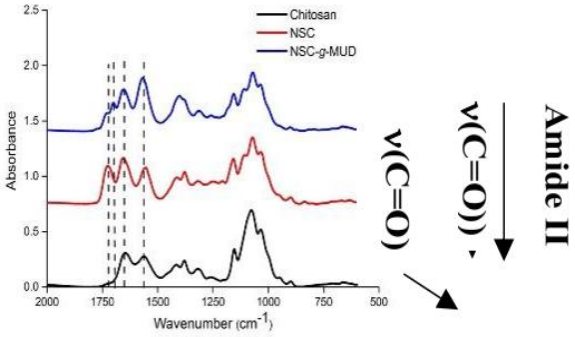

Figure 1: ATR-FTIR spectra of: (a) Chitosan, (b) *N*-Succinyl Chitosan and, (c) *N*-Succinyl Chitosan grafted with MUD on silicon substrates

The ATR-FTIR spectra of chitosan, N-Succinyl Chitosan (NSC), and NSC grafted with MUD showed significant differences, indicating successful modification. The spectrum of chitosan (black) displayed characteristic bands at 1561 cm^{-1} and 1645 cm^{-1}, corresponding to the amide II and amide I groups, respectively. The stretching vibrations were analyzed by determining the maximum peak values using Origin Pro 10 software, and the observed bands along with their corresponding molecular vibration assignments are summarized in Table 1.

The reaction of MUD-grafted NSC with the enzyme α-glucosidase releases the fluorogenic dye 4-methylumbelliferone (4-MU), which exhibits maximum emission at 450 nm when excited at 365 nm. To evaluate the fluorescence response of 4-MU at different pH levels, calibration experiments were performed in PBS buffer at pH 6.0, 7.0, and 8.0 using varying concentrations of the dye (1.0–5.0 µM). All PBS solutions were sterilized by autoclaving at 121°C before use, and fluorescence measurements were conducted using a fluorescence spectrometer and a microplate reader. The results showed that fluorescence intensity varied with both concentration and pH, confirming pH-dependent emission behavior of 4-MU. The corresponding fluorescence spectra obtained from these experiments are presented in Figures II (a,b,c).

Table 1: Peak Assignment of the Observed Bands in the ATR-FTIR Spectra of (a) Chitosan, (b) N-Succinyl Chitosan and, (c) N-Succinyl Chitosan Grafted with MUD on silicon substrates

Peak Assignment	Chitosan		NSC		NSC-g-MUD	
	Data	ref 84	Data	ref 3	Data	ref 3
(C=O) of carboxylic group (cm^{-1})	-	-	1727	1733	1727	1733
(C=O) of ester group (cm^{-1})	-	-	-	-	1700	1702
Amide I (cm^{-1})	1645	1620-1655	1656	1664	1653	1658
Amide II (cm^{-1})	1561	1550-1565	1555	1554	1569	1552

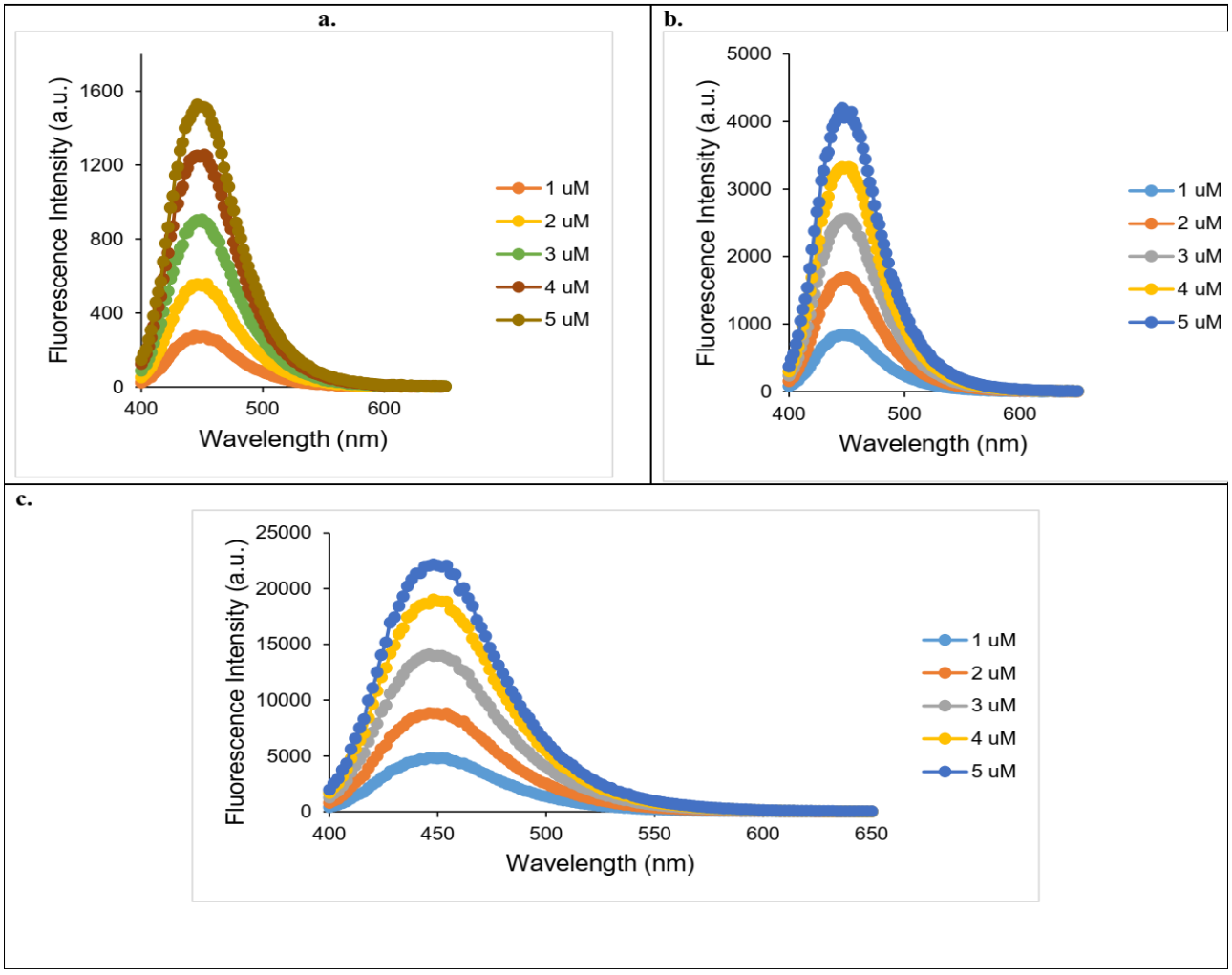

Figure II: Fluorescence spectra in microplate reader of different concentrations of 4-MU in PBS at varying pH values. (a) pH 6.0, (b) pH 7.0, and (c) pH 8.0; excitation at 365 nm

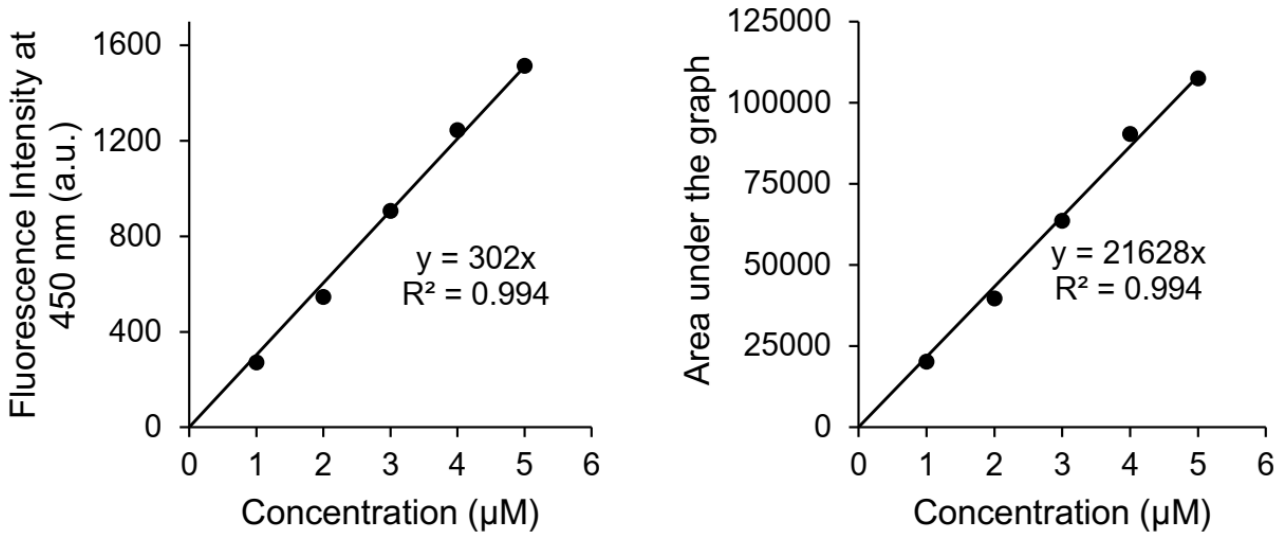

Figure III: Calibration plot of: (a) Fluorescence emission of 4-MU at different concentrations with emission maximum at 450 nm, and (b) Areas under the graphs of fluorescence spectra of 4-MU, in PBS at pH 6.0

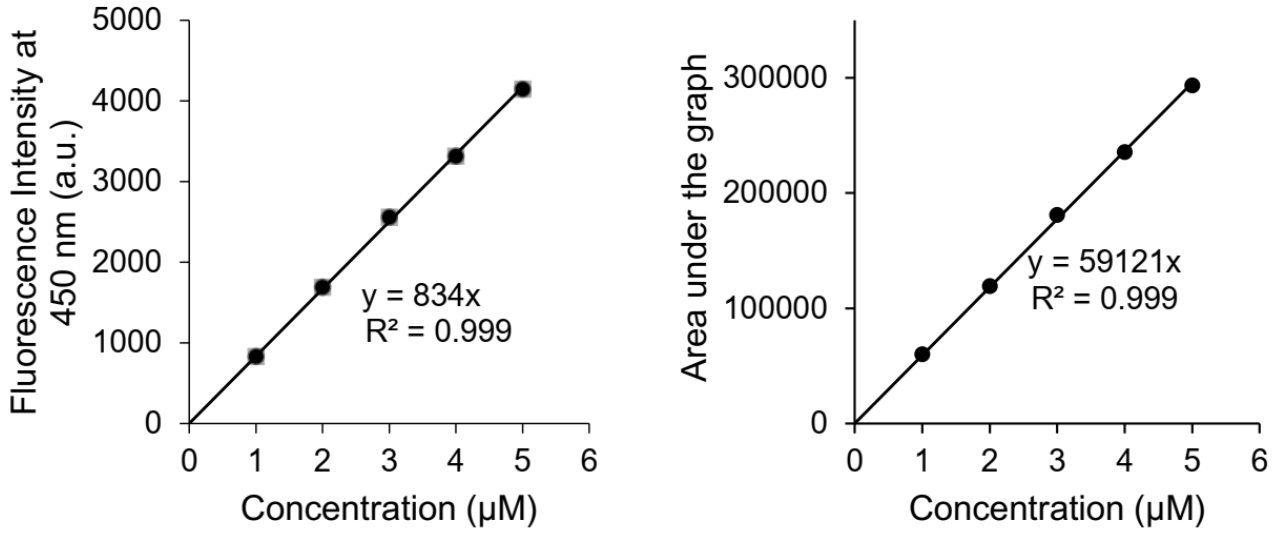

Figure IV: Calibration plot of: (a) Fluorescence emission of 4-MU at different concentrations with emission maximum at 450 nm, and (b) Areas under the graphs of Fluorescence Spectra of 4-MU, in PBS at pH 7.0

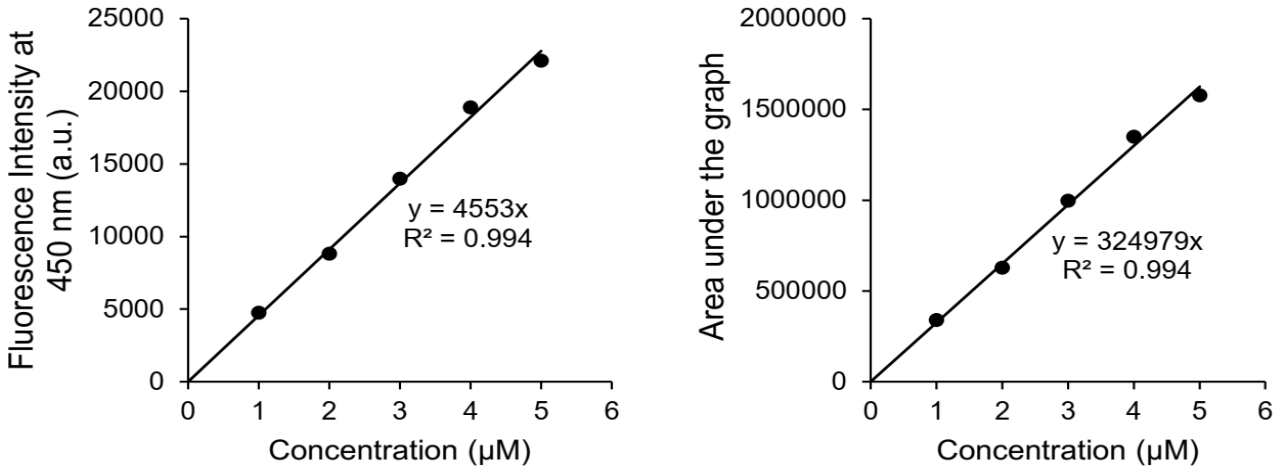

Figure V: Calibration plot of: (a) Fluorescence emission of 4-MU at different concentrations with emission maximum at 450 nm, and (b) Areas under the graphs of fluorescence spectra of 4-MU, in PBS at pH 8.0

The spectra were analyzed by plotting the maximum fluorescence response at 450 nm and the areas under the curves against dye concentration, as shown in Figures III(a), IV(a), and V(a). A consistent trend of increasing fluorescence intensity with higher 4-MU concentrations at fixed pH values was observed.

The resulting standard curve at pH 6.0 closely resembled that reported at pH 6.5 in previous studies, differing only in slope and intercept values. Similar patterns were also evident when analyzing the areas under the peaks, as presented in Figures III(b), IV(b), and VI(b).

Table 2 and Figure VI show that both the maximum fluorescence intensity of 5.0 µM 4-MU and the slope of the standard curve increase exponentially with rising pH.

Table 2: Values of Slopes of Standard Curves of 4-MU in the Microplate Reader at Different pH

pH	Slope of Standard Curve (a.u./□M)
6	302
7	834
8	4553

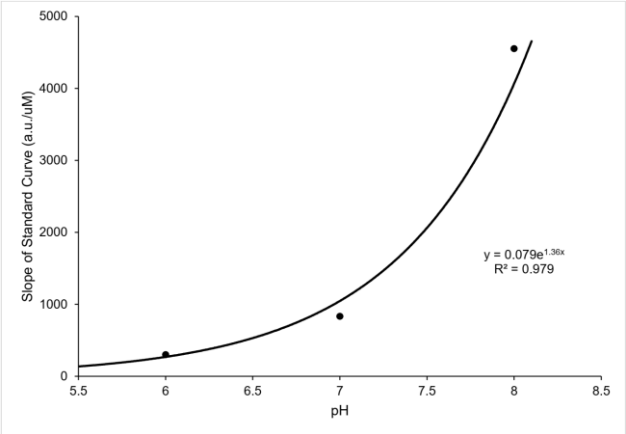

Figure VI: Graph showing the Effect of Increasing pH on the Fluorescence of 4-MU

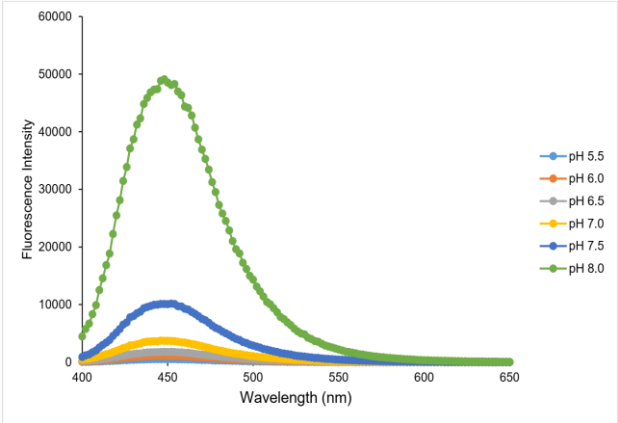

Figure VII: Fluorescence Spectra in a Microplate Reader of 5 µM 4-MU in PBS at Different pH values, excited at 365 nm

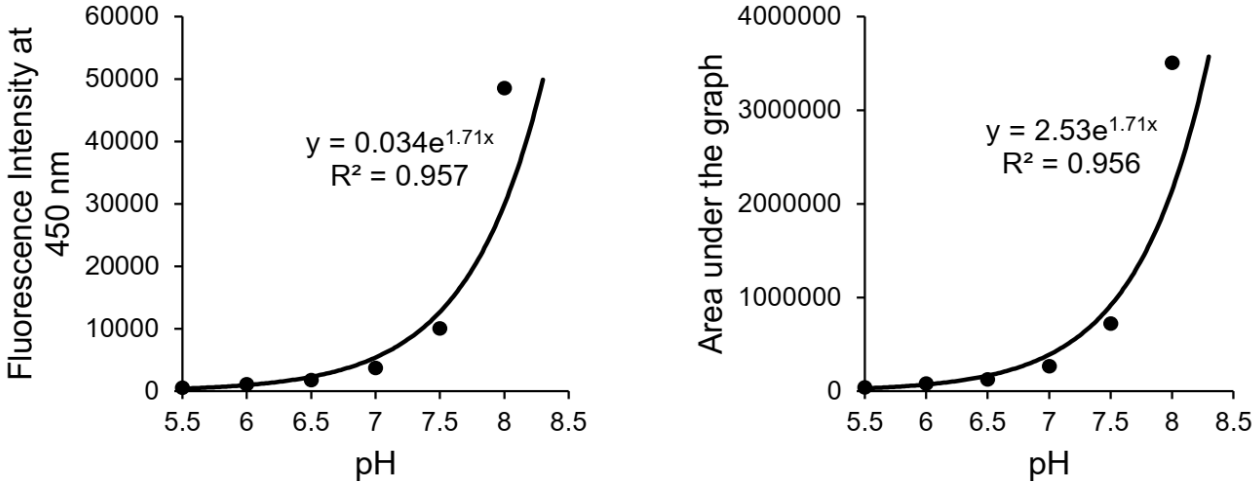

Figure VIII: Standard Curves from Microplate Reader showing: (a) Fluorescence emission of 5 µM 4-MU with Emission Maximum at 450 nm, and (b) Areas under the graphs of Fluorescence Spectra of 5 □M 4-MU in PBS at Different pH

Investigation of Response of 4-MU using Fluorescence Spectrometer: The fluorescence of 5 µM 4-MU in PBS was measured at different pH values using a microplate reader (Figures VII and VIII). The results show that fluorescence intensity increases exponentially with pH, being very low at pH 5.5–6.5 and significantly higher above pH 7, with maximum emission observed at pH 8. Both the emission peak at 450 nm and the areas under the curves confirm this trend.

The values in Table 3 below show that the slopes of the standard curves of 4-MU increase with an increase in pH. These values are plotted in the graph in Figure IX.

Table 3: Values of Slopes of Standard Curves of 4-MU in a Fluorescence Spectrometer at Different pH

pH	Slope of the standard curve
6	7.18
7	19.3
8	152

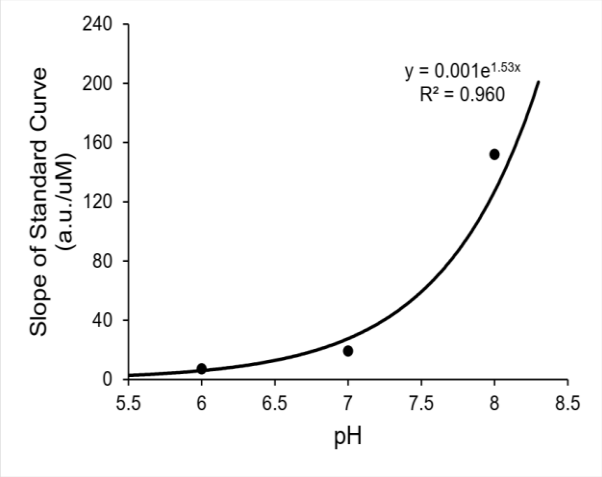

Figure IX: Graph showing the Effect of Increasing pH on the Fluorescence of 4-MU

Effect of Different pH Values on Fluorescence of 4-MU at Fixed Concentration: A 5 µM solution of 4-MU was prepared in PBS at different pH values, and its fluorescence was measured using a spectrometer. The spectra (Figure X) and standard curves (Figure XI) show that the fluorescence intensity of 4-MU increases exponentially as pH rises from 5.5 to 8.0, indicating a strong pH-dependent response.

Monitoring the Reaction of MUD-*g*-NSC with 0.2 µM α-GLU at Different pH: The enzymatic reaction of MUD-g-NSC with 0.2 µM α-glucosidase (α-GLU) was monitored at pH 6.0, 7.0, and 8.0 using a fluorescence spectrometer. The kinetics of 4-MU release were plotted against time in Figure XII, and the concentrations of 4-MU released were calculated using the calibration lines from previous measurements.

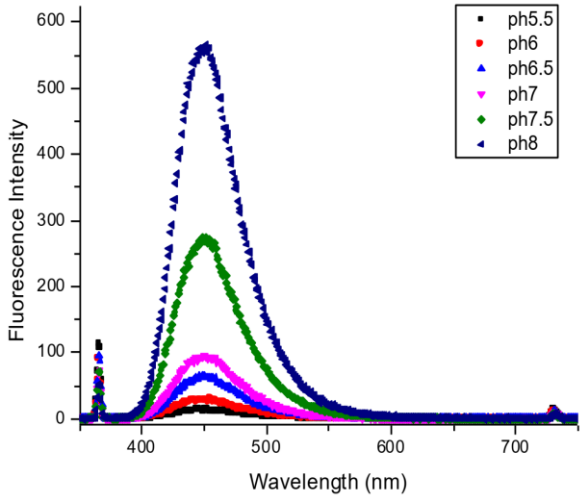

Figure X: Fluorescence spectra in a fluorescence spectrometer of 5.0 µM 4-MU in PBS at Different pH levels, excited at 365 nm

Table 4 shows that the highest concentration of 4-MU (20.6 µM) was released at pH 6.0, while the lowest (1.68 µM) was at pH 8.0. The reaction times required to reach maximum fluorescence were 150 min, 158 min, and 176 min at pH 6.0, 7.0, and 8.0, respectively. The kinetics of 4-MU production against time are shown in Figure XIII, indicating that the reaction proceeds fastest at pH 6.0 and slowest at pH 8.0.

Table 4: Concentrations of 4-MU Released During the Enzyme Reactions at Different pH Values

Equations of Calibration Lines Obtained	pH 6.0	pH 7.0	pH 8.0
	y = 7.18x	y = 19.3x	y = 152x
y (a.u.)	148	216	256
x (µM)	20.6	11.2	1.68
Time (min)	150	158	176

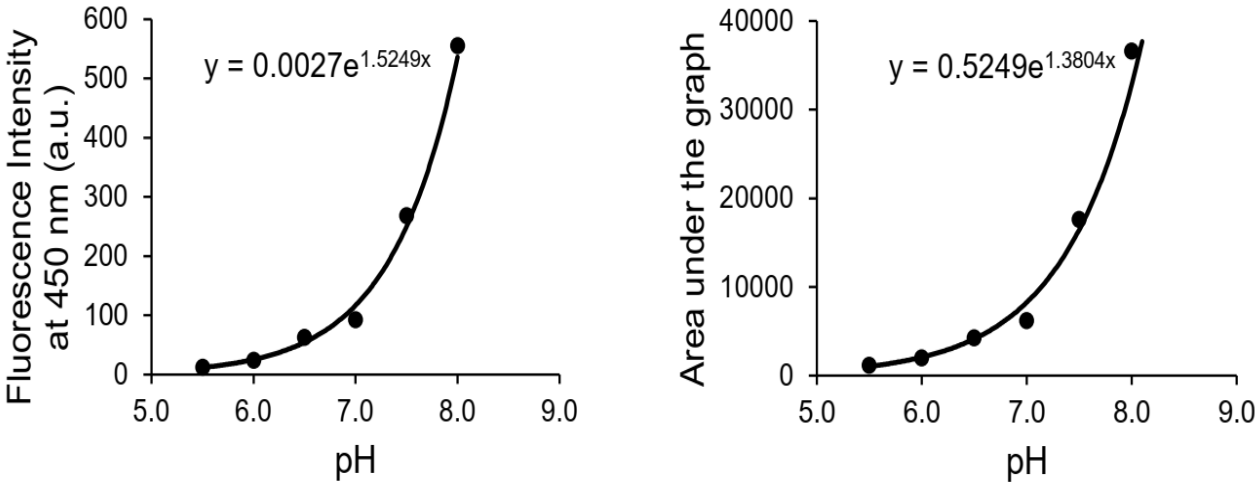

Figure XI: Standard Curves from Fluorescence Spectrometer showing: (a) Fluorescence emission of 5 µM 4-MU with Emission Maximum at 450 nm, and, (b) Areas under the graphs of Fluorescence Spectra of 5.0 □M 4-MU in PBS at Different pH

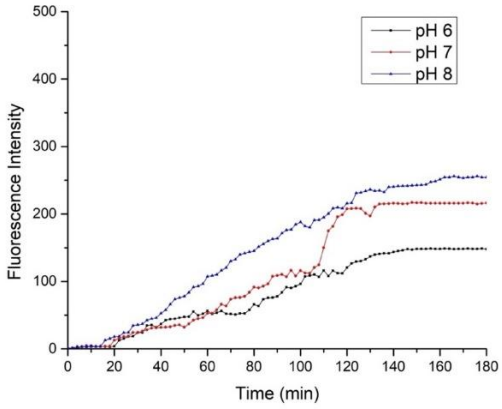

Figure XII: Kinetics of fluorescence of 4-MU produced against time of reaction between MUD-g-NSC and 0.2 µM α-GLU in PBS at Different pH

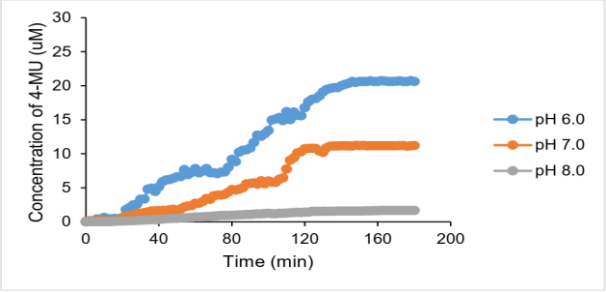

Figure XIII: Kinetics of Concentration of 4-MU Produced Against Time of Reaction between MUD-g-NSC and 0.2 µM α-GLU in PBS at Different pH

Calibration Experiments using the Chromogenic Dye: The NSC hydrogel grafted with X-GAL successfully reacted with β-GAL, releasing the blue dye 5,5′-dibromo-4,4′-dichloro-indigo. Wells with enzyme showed visible blue colour immediately after the reaction (fresh) and after 2 and 4 weeks of incubation at 37^0 C, while control wells with PBS showed no colour change. The intensity of the blue dye gradually decreased over time, indicating that the hydrogel retained enzymatic activity and stability throughout the 4 weeks (Figure XIV).

Absorbance Spectra of Aging of NSC Hydrogel Modified with X-GAL: The UV absorbance of the indigo dye released from NSC hydrogels grafted with X-GAL was measured in both sterilized and non-sterilized well-plates using a microplate reader, with background subtraction of PBS absorbance. Figure XV shows the absorbance spectra of the enzymatic reaction, indicating dye formation with peaks between 500–700 nm and a maximum at 650 nm.

Table 5 summarizes the UV absorbance and calculated theoretical dye concentrations over time. For the sterilized hydrogel, absorbance decreased from 0.109 (fresh) to 0.076 after 2 weeks and 0.061 after 4 weeks, corresponding to 30.4% and 44% dye loss, respectively. In contrast, the non-sterilized hydrogel showed smaller decreases: from 0.317 (fresh) to 0.298 after 2 weeks and 0.262 after 4 weeks, corresponding to 6% and 17.2% loss. This indicates that sterilization reduces both dye release

and hydrogel activity over time. Additionally, the non-sterilized hydrogel consistently exhibited higher absorbance, while some sterilized samples showed a shift in maximum absorbance from 650 nm to 600 nm.

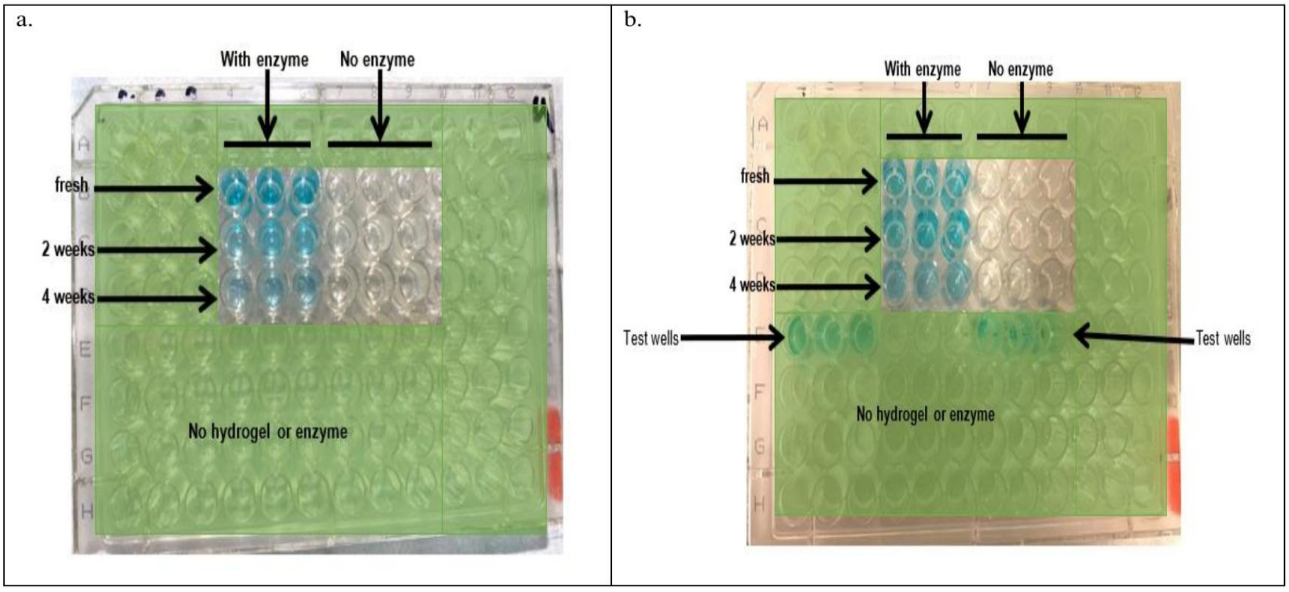

Figure XIV: (a) Sterilized and (b). Non-Sterilized Well-Plate after Enzyme Reaction in a Fresh State, after 2 weeks and 4 weeks

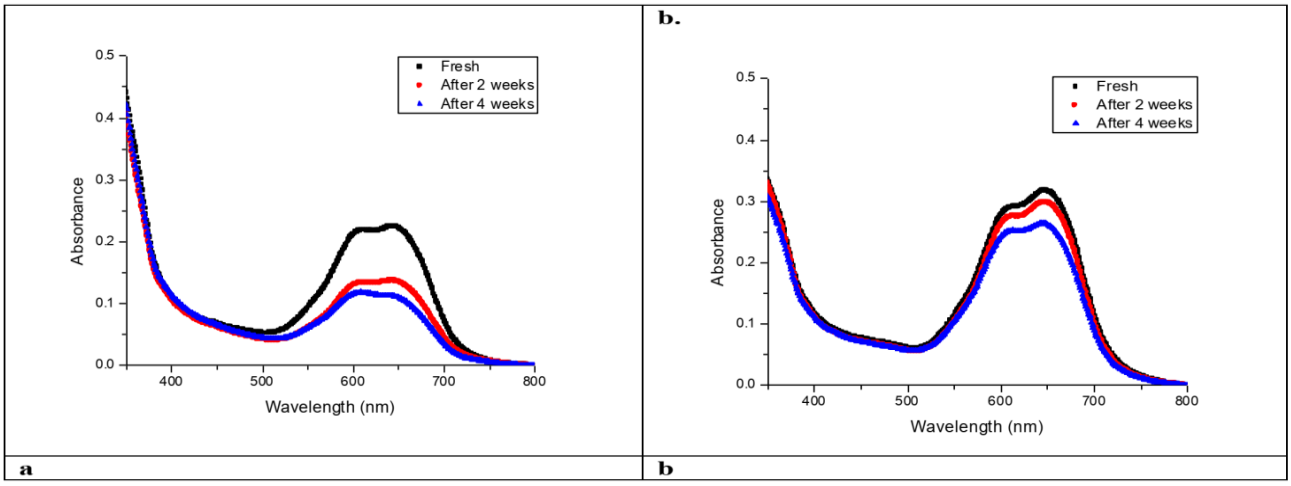

Figure XV: UV absorbance spectra of dimerized indigo during enzymatic reaction in β-GAL sensing hydrogels in a transparent 96 well-plate. (a) Sterilized hydrogel ([X-GAL]mod = 2.5 mmol/L, [β-Gal] = 0.2 µmol/L), (b) Non-sterilized hydrogel ([X-GAL]mod = 2.5 mmol/L, [β-Gal] = 0.2 µmol/L).

Table 5: UV Absorbance of Sterilized and Non-Sterilized Hydrogels in Fresh Condition and after 2 weeks and 4 weeks of Incubation at 37°C at Maximum Absorbance (wavelength of 650 nm)

Variables	UV Absorbance (units)		
	Fresh	After 2 weeks	After 4 weeks
Sterilized well plate	0.109	0.076	0.061
Theoretical Concentration of dye (mM)	2.50	1.74	1.40
% loss of dye	-	30.4	44.0

Variables	UV Absorbance (units)		
	Fresh	After 2 weeks	After 4 weeks
Non-sterilized well plate	0.317	0.298	0.262
Theoretical Concentration of dye (mM)	2.50	2.35	2.07
% loss of dye	-	6.00	17.2

Discussion

Chitosan hydrogel, widely used in drug delivery, wound dressing, and tissue engineering, can be improved through N-acylation to enhance its biocompatibility, solubility, and bioavailability. In this study, chitosan was modified to N-Succinyl Chitosan (NSC) via a nucleophilic ring-opening reaction with succinic anhydride, followed by purification with DMSO. NSC films were prepared on silicon wafers and 96-well plates, then modified with fluorogenic (MUD) or chromogenic (X-GAL) substrates[12]. Modification was achieved by EDC/NHS-mediated coupling, where EDC activates carboxyl groups of the substrate to form amine-reactive intermediates that bind to chitosan's amino groups, while NHS stabilizes the reaction. The resulting hydrogels were sensitized for enzyme detection — MUD-modified films for α-glucosidase (α-GLU) and X-GAL-modified films for β-galactosidase (β-GAL) — and characterized using ATR-FTIR .

The ATR-FTIR spectrum of NSC (red) presents a new strong peak at 1727 cm^{-1}, attributed to the symmetric stretching of the carboxylic group bond, confirming the successful introduction of succinyl groups to the primary amine groups of chitosan, forming amide bonds. Increased intensities at 1555 cm^{-1} and 1656 cm^{-1} further support amide bond formation. In the FT-IR spectra of NSC-g-MUD (blue), a new peak at 1700 cm^{-1} corresponds to symmetric stretching of the carboxyl group, while the decreased intensity at 1727 cm^{-1} indicates esterification reactions involving the carboxylic groups of NSC. These findings confirm successful modification reactions[13]. The spectrum of pure chitosan (black) shows characteristic amide II and amide I bands at 1561 cm^{-1} and 1645 cm^{-1}, respectively.

The spectra illustrate the effect of different concentrations of 4-MU in PBS at pH 6.0, 7.0, and 8.0, showing consistent maximum emission peaks at 450 nm. Increasing 4-MU concentration results in proportional increases in fluorescence intensity, demonstrating a concentration-dependent fluorescence response. Calibration plots reveal a linear relationship between fluorescence response and 4-MU concentration up to 5.0 μM, with regression lines passing through the origin. Linear equations ($y = mx$) and R^2 values confirm strong correlation and reproducibility. These results align with previous literature[13,14], where similar linear fluorescence-concentration relationships were observed at pH 6.5. The increased fluorescence intensity with rising dye concentration is attributed to a greater number of dye molecules per unit area, producing stronger detectable fluorescence signals.

The slope of the 4-MU standard curve increases exponentially with pH, indicating a higher fluorescence response rate at elevated pH values. This demonstrates that 4-MU fluorescence is pH-sensitive, with lower fluorescence under acidic conditions due to predominance of the phenolic form and higher fluorescence under alkaline conditions due to the phenoxide form. The observed pH-dependent fluorescence supports this equilibrium shift, consistent with reports that maximum emission occurs around pH 10, where the phenoxide form dominates.

Fluorescence measurements of 4-MU (1–5 μM) at pH 6.0, 7.0, and 8.0 (Figure VII) consistently showed a maximum emission at 450 nm, with intensity increasing proportionally with concentration. Calibration plots (Figure VIII) confirmed linearity between emission intensity and concentration, ensuring accuracy and reproducibility. The slopes of these standard curves increased exponentially from 7.18 at pH 6.0 to 152 at pH 8.0, confirming that higher pH enhances 4-MU fluorescence. This pattern matched microplate reader results, validating instrument consistency. The fluorescence enhancement is driven by the phenolic–phenoxide equilibrium: the phenolic form predominates at low pH with weak emission, whereas the phenoxide form dominates at high pH with stronger fluorescence. These findings confirm the pH sensitivity of 4-MU, reinforcing its suitability as a fluorogenic substrate for enzyme assays. The enzymatic reaction of MUD-g-NSC with 0.2 μM α-GLU exhibited distinct pH-

dependent behavior. The highest release of 4-MU (20.6 µM) occurred at pH 6.0 within 150 minutes, while the lowest release (1.68 µM) occurred at pH 8.0 after 176 minutes. These results indicate optimal α-GLU activity near pH 6.0, with decreasing activity at higher pH levels, consistent with known α-glucosidase enzyme profiles[15]. The kinetic data confirm that MUD-g-NSC efficiently converts to 4-MU under slightly acidic conditions.

NSC hydrogels grafted with X-GAL retain enzymatic functionality for at least four weeks. Persistent blue coloration in β-GAL–treated wells indicates continued enzymatic activity, while gradual fading suggests mild hydrogel aging or reduced substrate accessibility, without loss of detection ability. These findings confirm the structural and functional stability of NSC-g-X-GAL hydrogels for long-term enzyme detection applications. Sterilization significantly influenced hydrogel stability and enzymatic response. The sterilized hydrogel exhibited more than twice the dye loss of non-sterilized samples over four weeks, reflecting reduced enzymatic activity. This may be due to gamma sterilization partially breaking ester bonds between X-GAL and NSC or weakening the crosslinked network, lowering substrate availability and dye retention. A shift in absorbance maxima in sterilized samples suggests structural alterations within the hydrogel matrix. Overall, non-sterilized hydrogels preserved higher enzymatic activity and stability, confirming that sterilization adversely impacts hydrogel integrity and functional performance.

Conclusion

Chitosan hydrogels were successfully modified with fluorogenic (MUD) and chromogenic (X-GAL) substrates, demonstrating effective covalent attachment and enzymatic responsiveness. MUD-modified hydrogels exhibited optimal enzymatic activity at pH 6.0, confirming enzyme-specific cleavage, while X-GAL-modified hydrogels retained activity for up to four weeks, indicating good stability and durability. These findings highlight the potential of modified chitosan hydrogels as a versatile and reliable platform for the rapid and specific detection of bacterial enzymes. Their adaptability with various substrates and stability under different conditions make them promising candidates for applications in medicine, food safety, and water quality monitoring. Further studies on pH dependence and optimization of reaction conditions could enhance their efficiency and broaden their practical applications.

Acknowledgements
None

Conflict of Interest
None

Financial Disclosure
None

Authors' contributions
Conceptualization: Kausain Akther, Md Al Amin; Data curation: Kausain Akther, Aminul Islam, Fariya Khan Sharna; Formal analysis: Kausain Akther, Anika Zafreen; Project administration: Md Al Amin, Md Samiul Bashir; Supervision: Md Al Amin, Md. Ashiqur Rahman, Md Samiul Bashir; Visualization: Fariya Khan Sharna, Aminul Islam, Arifa Akram; Writing – original draft: Kausain Akther, Md Al Amin; Writing – review & editing: Md. Ashiqur Rahman, Anika Zafreen, Arifa Akram;

Data Availability
Any inquiries regarding supporting data availability of this study should be directed to the corresponding author and are available from the corresponding author on reasonable request.

Ethics Approval and Consent to Participate
The Institutional Review Board granted the study ethical approval. Since this was a prospective study, every study participant provided formal informed consent. Each method followed the appropriate rules and regulations.

How to cite this article: Akther K, Amin MA, Sharna FK, Islam A, Bashir MS, Zafreen A, Rahman MA, Akram A. Development and Evaluation of Fluorogenic and Chromogenic Chitosan-Based Hydrogels for the Detection of Bacterial Enzymes. Bangladesh J Infect Dis 2025;12(2):273-284

ORCID
Kausain Akther: https://orcid.org/0009-0006-3528-0542
Md. Al Amin: https://orcid.org/0009-0006-6377-5358
Fariya Khan Sharna: https://orcid.org/0009-0001-7562-6409
Aminul Islam: https://orcid.org/0009-0002-8431-3604
Md. Samiul Bashir: https://orcid.org/0009-0001-7295-1329
Anika Zafreen: https://orcid.org/0009-0000-3222-7830
Md. Ashiqur Rahman: https://orcid.org/0000-0002-9430-5547
Arifa Akram: https://orcid.org/0000-0001-8829-9817

Article Info
Received on: 1 September 2025
Accepted on: 20 October 2025
Published on: 1 December 2025

References

1. Sadat Ebrahimi MM, Schönherr H. Enzyme-sensing chitosan hydrogels. Langmuir. 2014;30(26):7842-50.

2. Öhlknecht C, Tegl G, Beer B, Sygmund C, Ludwig R, Guebitz GM. Cellobiose dehydrogenase and chitosan-based lysozyme responsive materials for antimicrobial wound treatment. Biotechnology and Bioengineering. 2017;114(2):416-22.
3. Alhussaini MS, Alyahya AA, Al-Ghanayem AA. Chitosan-Based Materials for the Fluorescence and Colorimetric Detection of Pathogenic Bacteria: A Comprehensive Review (2011–2025). Critical Reviews in Analytical Chemistry. 2025:1-9.
4. Jia Z, Müller M, Schönherr H. Towards multiplexed bacteria detection by enzyme responsive hydrogels. InMacromolecular Symposia 2018;379(1):1600178
5. Eivazzadeh-Keihan R, Noruzi EB, Mehrban SF, Aliabadi HA, Karimi M, Mohammadi A, Maleki A, Mahdavi M, Larijani B, Shalan AE. The latest advances in biomedical applications of chitosan hydrogel as a powerful natural structure with eye-catching biological properties. Journal of Materials Science. 2022;57(6):3855-91.
6. Jia Z, Sukker I, Müller M, Schönherr H. Selective discrimination of key enzymes of pathogenic and nonpathogenic bacteria on autonomously reporting shape-encoded hydrogel patterns. ACS Applied Materials & Interfaces. 2018;10(6):5175-84.
7. Pires NM, Dong T, Hanke U, Hoivik N. Recent developments in optical detection technologies in lab-on-a-chip devices for biosensing applications. Sensors. 2014;14(8): 15458-79
8. Layek B, Singh J. Amino acid grafted chitosan for high performance gene delivery: comparison of amino acid hydrophobicity on vector and polyplex characteristics. Biomacromolecules. 2013;14(2):485-94
9. da Costa SG, Bates P, Dillon R, Genta FA. Characterization of α-glucosidases from Lutzomyia longipalpis reveals independent hydrolysis systems for plant or blood sugars. Frontiers in Physiology. 2019;10:248.
10. Wu S, Wu S, Zhang X, Feng T, Wu L. Chitosan-based hydrogels for bioelectronic sensing: recent advances and applications in biomedicine and food safety. Biosensors. 2023;13(1):93.
11. Lv S, Liang S, Zuo J, Zhang S, Wei D. Preparation and application of chitosan-based fluorescent probes. Analyst. 2022;147(21):4657-73.
12. Kaur K, Schoenherr H. Enzyme-responsive chitosan-based electrospun nanofibers for enhanced detection of β-glucuronidase from pathogenic E. coli. Polymer. 2025;317:127896.
13. Kaur K, Chelangat W, Druzhinin SI, Karuri NW, Müller M, Schönherr H. Quantitative E. coli enzyme detection in reporter hydrogel-coated paper using a smartphone camera. Biosensors. 2021;11(1):25.
14. Hu M, Tang Y, He X, Liu K, Qin L, Wang X, Wang Q. Enzyme-Integrated Hydrogels for Advanced Biological Applications. Polymer Science & Technology. 2025.
15. Jia Z, Müller M, Le Gall T, Riool M, Müller M, Zaat SA, Montier T, Schönherr H. Multiplexed detection and differentiation of bacterial enzymes and bacteria by color-encoded sensor hydrogels. Bioactive materials. 2021;6(12):4286.